ECCOMAS Congress 2016
VII European Congress on Computational Methods in Applied Sciences and Engineering
M. Papadrakakis, V. Papadopoulos, G. Stefanou, V. Plevris (eds.)
Crete Island, Greece, 5–10 June 2016

INVERSION METHODS BASED ON KALMAN FILTERING FOR IDENTIFICATION IN TUNNELING PROBLEMS

Tamara Nestorović[1] **and Luan T. Nguyen**[1]

[1]Ruhr-Universität Bochum, Mechanics of Adaptive Systems
Universitätsstr. 150, 44801 Bochum, Germany
e-mail: {Tamara.Nestorovic,Thanh.Nguyen-w7t}@rub.de

Keywords: Inversion methods, Kalman filter, Parameter estimation.

Abstract. *In this study we present an overview of the inversion methods based on the Kalman filtering technique, which was implemented for the identification of geological structure ahead of the underground tunnel. The methodology is particularly aimed at solving for model parameters even in the presence of noisy environment (measurements). One of the main goals of this investigation is related to the advance of the tunnel boring machine (TBM) during excavation in unknown environment in order to mitigate the excavation risks due to unpredicted obstacles and reduce costs caused by the TBM stoppage during tunneling under uncertain soil conditions. The inversion methods are implemented for the purpose of the reconnaissance in mechanized tunneling.*

Several inversion methods are investigated and implemented. The Kalman filter as parameter estimator, already having been successfully implemented in control systems, has been introduced here also for the purpose of geotechnical parameters estimation. Since the Kalman filter was originally developed for linear systems primarily represented in the state space form, the implementation with the geotechnical soil models was limited by the nonlinearities. Therefore modifications of the Kalman filter have been introduced and implemented, such as extended Kalman filter (EKF), sigma-point Kalman filter (SPKF) and unscented Kalman filter (UKF). The extended Kalman filter local iteration procedure incorporated with finite element analysis software has been used for identification of the soil parameters using tunneling induced deformations under assumptions of existing surface pressure load and an obstacle ahead of the tunnel face. The identification is performed based on the numerically generated noisy measurements. The inherent linearization in the extended Kalman filter makes it difficult to implement and it is reliable only for slightly nonlinear system models. Therefore the further improvement of the inversion method has been done by combining the EKF with the derivativeless deterministic sampling-based approximation where a set of deterministically sampled points, called sigma points, can be used to represent the mean and covariance of the estimated quantities. The update mechanisms are inherited from the linear Kalman filter. For the purpose of the full seismic waves inversion for predicting ahead of the underground tunnel a new hybridized global optimization method that combines the simulated annealing global search with unscented Kalman filter minimization has been proposed. The implementation of the inversion methods has been shown on several numerical examples.

1 INTRODUCTION

From the optimization point of view, inverse methods can generally be considered as a solution of the optimization problem, mainly through minimization of certain objective function. Implementation of the inversion methods in different fields of research and engineering plays an important role. One demanding implementation field is the reconnaissance in mechanized tunneling. Identification of the soil parameters ahead of the tunnel front, in order to predict possible obstacles, layer changes or similar anomalies can contribute to considerable savings by avoiding the damages or unplanned stoppage of the tunnel boring machine (TBM). Inversion methods for parameter estimation based on Kalman filters represent a promising tool for such applications.

The Kalman filter method was developed by Rudolf E. Kalman in early 1960s [1] and was originally aimed at implementations in control of dynamics systems and signal processing. In recent years, some applications of the Kalman filter method have also arisen in the field of geotechnical engineering for estimation of material parameters [2, 3, 4, 5]. Originally the Kalman filter was developed as dynamic least square states estimator for systems represented by linear models in the state space form. A modification of the approach with application in geotechnical engineering uses quasi-static models since the geotechnical parameters are static over the considered estimation time frame. Thus, a stationary transition of state estimates is suitable for this purpose [2].The procedure starts from a priori estimates and utilizes a set of measurement data to calculate a posteriori estimates. Means and covariances of the quantities being estimated are repeatedly updated so that the variance of the estimation error is reduced until convergence of the estimated quantities to unbiased true state and model parameters is reached [1, 6]. In this paper several techniques relying on modifications of Kalman filter are presented and implemented for the estimation of parameters in geotechnical models. The methodology is documented by several numerical examples.

2 KALMAN FILTER BASED METHODS

Quasi-stationary representation of a geotechnical model can be generally expressed in the form of a nonlinear state space matrix equation

$$\mathbf{d} = \mathbf{h}(\mathbf{x}, \mathbf{m}, \mathbf{f}) \tag{1}$$

where $\mathbf{d}$ stores modeling outputs obtained from the model $\mathbf{h}(\cdot)$ (usually a finite element – FE model), $\mathbf{x}$ is the current physical state of the model, $\mathbf{m}$ contains the model parameters (for example material parameters), and $\mathbf{f}$ represents external loads including the boundary conditions. When it is assumed that the applied loads and the initial and boundary conditions are properly determined, the identification problem consists of determining the actual model parameters $\mathbf{m}$. A frequent problem is the model calibration by inverse analysis in order to match the model outputs $\mathbf{d}$ to the in-situ measurement or laboratory tests measurement data $\mathbf{d}^{obs}$. This matching can be expressed in terms of optimization of a certain objective function, i.e. minimization of the required misfit. Arising problems such as high nonlinearity of the geotechnical models, time consuming forward calculations of the models and uncertainty of the measurement data require special treatment and adaptation of the identification methods to these requirements. The Kalman filter based methods which meet those requirements are presented in the following sections.

2.1 Extended Kalman Filter

The quasi-stationary model of Eq. 1 can be represented in terms of the state transition 2a and the output 2b equations:

$$\mathbf{m}_k = \mathbf{m}_{k-1} + \mathbf{w}_{k-1}, \tag{2a}$$

$$\mathbf{d}_k = \mathbf{h}\left(\mathbf{m}_k\right) + \mathbf{v}_k, \tag{2b}$$

where vector $\mathbf{m}_k$ contains the model parameters and $\mathbf{x}_k$ is the physical state of the model at recursive step t_k. Vector $\mathbf{d}$ extracts modeling outputs at predefined positions in the model from the modeling observation Eq. 2b. In Eq. 2a, the stationary process transition is added by a modest amount of pseudo-noise $\mathbf{w}_k$ to act like parameter updating from one iterative step to the next. Inexactness of the modeling observation function $\mathbf{h}(\cdot)$ in Eq. 2b is characterized by an amount of uncertainty $\mathbf{v}_k$. Additive uncertainties $\mathbf{w}_k$ and $\mathbf{v}_k$ are assumed to be uncorrelated and white Gaussian having zero-mean and time-invariant covariance matrices $\mathbf{Q}$ and $\mathbf{R^m}$ respectively.

In the Kalman filter algorithm the mean and error covariance of the state are propagated through time. These mean and error covariance of the state are updated every time new measurements arise [7]. The time update equations of the mean and covariance of the state are calculated in the following way:

$$\hat{m}_k^- = \hat{m}_{k-1}^+; P_k^- = P_{k-1}^+ + Q, \tag{3}$$

where $\hat{m}_k = E(m_k)$ represents the mean (mathematical expectation) of the state and $P_k = E\left[(m_k - \hat{m}_k)(m_k - \hat{m}_k)^T\right]$ is the covariance matrix at *k*-th iteration. The superscript '–' denotes *a priori* estimate, i.e. the estimate before measurement is available, whereas the superscript '+' denotes *a posteriori* estimate after the measurement is taken into account. At the time t_k in the local iterative loop i of the extended Kalman filter, the Kalman gain $K_{k,i}$, the measurement updates of the state estimate $\hat{m}_{k,i+1}^+$ and the estimation error covariance matrix $P_{k,i+1}^+$ are iterated according to the following equations.

$$\begin{aligned}
H_{k,i} &= \left.\frac{\partial h}{\partial m}\right|_{\hat{m}_{k,i}^+} \\
K_{k,i}^g &= P_k^- H_{k,i}^T (H_{k,i} P_k^- H_{k,i}^T + R)^{-1} \\
P_{k,i+1}^+ &= (I - K_{k,i}^g) P_k^- \\
\hat{m}_{k,i+1}^+ &= \hat{m}_k^- + K_{k,i}^g \left[d_{exp} - h(\hat{m}_{k,i}^+, 0) - H_{k,i}(\hat{m}_k^- - \hat{m}_{k,i}^+)\right]
\end{aligned} \tag{4}$$

Here H represents the sensitivity matrix (observation derivative matrix with respect to the state estimate), K^g is the Kalman gain and d_{exp} is expected measurement. The sensitivity matrix is calculated for each global iteration k and local iteration i as

$$H_{m,n} = \frac{\partial h_m}{\partial m_n} = \frac{h_m(\mathbf{m} + \Delta m_n \mathbf{e}_n) - h_m(\mathbf{m})}{\Delta m_n} \tag{5}$$

where h_m is the *m*-th element of observation vector, m_n is the *n*-th element of the parameter vector and Δm_n is a small increment of the *n*-th element of parameter vector. The unit vector $\mathbf{e}_n$ has value one in *n*-th element and zeros elsewhere. The estimation algorithm is coupled with the finite element analysis (FEA) software. An independent treatment of FEA program represents a significant advantage of the proposed method, in the sense that any FEA program can be

incorporated into the process when the communicative interface between the main algorithm flow and the FEA program has been created. In order to begin the filter process, an initial value for state vector x_0 and its corresponding estimation error covariance matrix P_0 are assigned. Usually, initial state vector contains the most likely values of parameters of the system that can be inferred from prior knowledge or preliminary geomechanical tests. The estimation error covariance matrix gives information about the confidence of the initial parameter values. The procedure is to locally iterate the filtering process on the first set of data in order to assess the information inherent to the data. Then, the second set of data is processed to filtering and is similarly iterated, and so on. The iterative process will continue until a stop criterion is met, which may be *i*) convergence of the cost function to he predefined minimal values, *ii*) absolute value of the two successive estimates is less than a predefined tolerance or *iii*) the specified number of iterations. In this method, the error covariance matrix of estimation P_k is enlarged with a modification weight in every global iteration to obtain fast convergence.

2.2 Sigma-Point Kalman Filter

Due to inherent linearization the EKF is related with implementation difficulties, and in addition this state estimation method has limitations in implementation with highly nonlinear models. Therefore alternative types of the Kalman filter for nonlinear models have been developed, which obviate the need for linearization of the state-space model, like the unscented Kalman filter [8]. Later, [9] has combined and systematized this new filter together with some other independent works that derived the derivativeless deterministic sampling based approximation of the Gaussian statistics to belong to the family of SPKF. This family of the Kalman filter is based on the principle that a set of deterministically sampled points, called sigma-points, can be used to represent the mean and covariance of the estimated quantities. Update mechanisms are inherited from the linear Kalman filter [1].

The sigma-points consist of $2n + 1$ discretely distributed points around the current estimate on the n-dimension space. The distribution of these sigma-points around the current estimate is determined by square-root decomposition of the prior covariance and the spread of them can be assigned by setting a scaling parameter ζ as follows.

$$\boldsymbol{\sigma} = \zeta\sqrt{\mathbf{P}_{k-1}}, \tag{6}$$

$$(\boldsymbol{\mathcal{M}}_{k-1})_0 = \hat{\mathbf{m}}_{k-1}, \tag{7}$$

$$(\boldsymbol{\mathcal{M}}_{k-1})_i = \hat{\mathbf{m}}_{k-1} + (\boldsymbol{\sigma})_i, \text{ for i = 1:n} \tag{8}$$

$$(\boldsymbol{\mathcal{M}}_{k-1})_{i+n} = \hat{\mathbf{m}}_{k-1} - (\boldsymbol{\sigma})_i, \text{ for i = 1:n} \tag{9}$$

where the scaling parameter is calculated as $\zeta = \sqrt{n + \lambda}$. The parameter λ remains free to tune. It is suggested to select $n + \lambda = 3$ when $\mathbf{m}$ is assumed Gaussian [8]. The notation $(\cdot)_i$ denotes the i-column of the matrix within parentheses.

Each sigma-point is associated with a weight. The weights are defined as in Eq. 16 such that the sum of weights is unity.

$$W_0 = \frac{\lambda}{n+\lambda}, W_i = W_{i+n} = \frac{1}{2(n+\lambda)}, \text{ for i = 1:n} \tag{10}$$

Direct nonlinear transfer of the sigma-points through the nonlinear state-space functions helps reserve second order accuracy of the Gaussian approximate estimated quantities as opposed to first order truncation of the Taylor series employed by the EKF. In addition, the minimization

of the objective misfit function Eq. 11 should be provided.

$$S(\mathbf{m}_k) = \frac{1}{2}\left((\mathbf{h}(\mathbf{m}_k) - \mathbf{d}^{obs})^t \mathbf{R}^{-1}(\mathbf{h}(\mathbf{m}_k) - \mathbf{d}^{obs}) + (\mathbf{m}_k - \hat{\mathbf{m}}_{k|k-1})^t \mathbf{P}^{-1}_{k|k-1}(\mathbf{m}_k - \hat{\mathbf{m}}_{k|k-1})\right) \tag{11}$$

The recursive prediction step and correction step of the SPKF are summarized in Algorithm 1.

Algorithm 1: The SPKF algorithm for parameter identification

Initialization:

$$\begin{aligned} \hat{\mathbf{m}}_0 &= \mathbf{m}^{prior} \\ \mathbf{P}^m_0 &= \mathbf{P}^{prior} \end{aligned}$$

$k \leftarrow 1$

while S *(Eq. 11)* $< TOLERANCE$ **do**

Prediction step:

Generate the sigma-points Eq. 6-9:$(\boldsymbol{\mathcal{M}}_{k-1})_i$

$$(\boldsymbol{\mathcal{M}}_{k|k-1})_i = (\boldsymbol{\mathcal{M}}_{k-1})_i$$

$$\hat{\mathbf{m}}_{k|k-1} = \sum_{i=0}^{2n} W_i (\boldsymbol{\mathcal{M}}_{k|k-1})_i$$

$$\mathbf{P}^m_{k|k-1} = \sum_{i=0}^{2n} W_i \left((\boldsymbol{\mathcal{M}}_{k|k-1})_i - \hat{\mathbf{m}}_{k|k-1}\right)\left((\boldsymbol{\mathcal{M}}_{k|k-1})_i - \hat{\mathbf{m}}_{k|k-1}\right)^t + \mathbf{Q}$$

$$(\boldsymbol{\mathcal{D}}_{k|k-1})_i = \mathbf{h}\left((\boldsymbol{\mathcal{M}}_{k|k-1})_i\right)$$

$$\hat{\mathbf{d}}_{k|k-1} = \sum_{i=0}^{2n} W_i (\boldsymbol{\mathcal{D}}_{k|k-1})_i$$

$$\mathbf{P}^d_{k|k-1} = \sum_{i=0}^{2n} W_i \left((\boldsymbol{\mathcal{D}}_{k|k-1})_i - \hat{\mathbf{d}}_{k|k-1}\right)\left((\boldsymbol{\mathcal{D}}_{k|k-1})_i - \hat{\mathbf{d}}_{k|k-1}\right)^t + \mathbf{R}$$

$$\mathbf{P}^{md}_{k|k-1} = \sum_{i=0}^{2n} W_i \left((\boldsymbol{\mathcal{M}}_{k|k-1})_i - \hat{\mathbf{m}}_{k|k-1}\right)\left((\boldsymbol{\mathcal{D}}_{k|k-1})_i - \hat{\mathbf{d}}_{k|k-1}\right)^t$$

Correction step:

$$\begin{aligned} \mathbf{K}_k &= \mathbf{P}^{md}_{k|k-1}(\mathbf{P}^d_{k|k-1})^{-1} \\ \hat{\mathbf{m}}_k &= \hat{\mathbf{m}}_{k|k-1} + \mathbf{K}_k\left(\mathbf{d}^{obs} - \hat{\mathbf{d}}_{k|k-1}\right) \\ \mathbf{P}^m_k &= \mathbf{P}^m_{k|k-1} - \mathbf{K}_k \mathbf{P}^d_{k|k-1}\mathbf{K}^t_k \end{aligned}$$

$k \leftarrow k + 1$

end

In this Algorithm, the means of predicted parameters and model outputs are calculated as weighted summation over the sigma-points and the corresponding predicted model outputs.

The predicted model outputs $\boldsymbol{\mathcal{D}}_{k|k-1}$ are the results of direct nonlinear transfers of the representative sigma-points $\boldsymbol{\mathcal{M}}_{k|k-1}$ through the nonlinear model function $\mathbf{h}(\cdot)$. The predicted estimation error covariances of the estimated parameters $\mathbf{P}^m$, of the model outputs $\mathbf{P}^d$, and of the cross-covariance between them $\mathbf{P}^{md}$ are calculated as weighted summation of the squares of distances between each sigma-point and respective model output to the corresponding mean estimates. The correction equations for the SPKF take into account the means and covariances approximated using the sigma-points and the nonlinear model outputs in the prediction step without need for calculation of the Jacobians.

For application in calibration of FE model in geomechanics, value for each parameter can be limited to a certain range depending on initial categorization of geomaterial samples. Therefore, it is advantageous to apply a feasible range for each parameter in the identification process. The advantage of giving constraints to the parameter space is threefold: *i*) it helps to exclude the unreasonable convergence points, which are local minima, of the objective function, *ii*) it allows the FE code to run uninterruptedly during the iterative estimation process as the parameters are clipped in the reasonable regions, and *iii*) it may help to accelerate the estimation process by filtering algorithms since the estimation bias is not allowed to explode. Here, the 'clipping' constraints handling for both the EKF and the SPKF described in [10] is applied.

2.3 Unscented Kalman Filter

The UKF is a very successful state and parameter estimator for nonlinear dynamic models in which the posterior estimates are inferred from noisy observation data. It aims to overcome the inherent limitations of the traditional extended Kalman filter that works only for slightly nonlinear models and requires linearization of the nonlinear models. This filter belongs to the sigma-point Kalman filter family, and represents a derivative-free estimator for nonlinear state-space models that can be efficiently adapted for solving parameter identification of static and dynamic models [9].

The forward model is described in a similar form as in Eq. 2b. In this case **d** stores the model outputs at r observation points resulting from the nonlinear model **h**. For time-dependent problem such as wave propagation, the model $\mathbf{h}(\cdot)$ is solved in time steps for the simulation period; and the resulting batch data are stored in **d**. The modeling error **v** is caused by assumptions made in building the mathematical model and numerical approximations. This error can be assumed to be zero-mean Guassian distribution with covariance $\boldsymbol{R}$. The misfit s to be minimized is constructed for each output measurement j by squares of differences between the measured data $d^{obs}(t)$ and the modeled outputs $d(t)$ in the time window of interest $[0, \tau]$:

$$s_j = \frac{1}{2}\int_0^{\tau} \|d_j^{obs}(t) - d_j(\boldsymbol{m}, t)\|^2 dt, j \in \{1, 2, .., r\}. \tag{12}$$

The predicted mean and covariance before measurement update are denoted as $\hat{\boldsymbol{m}}$ and $\boldsymbol{P}^m$ respectively. If n model parameters are to be estimated, $2n + 1$ sigma-points are defined as follows for the unscented transformation to approximate a Gaussian distribution of the predicted estimate centered at $\hat{\boldsymbol{m}}$ with covariance $\boldsymbol{P}^m$:

$$\boldsymbol{\mathcal{M}}_0 = \hat{\boldsymbol{m}}, \tag{13}$$

$$\boldsymbol{\mathcal{M}}_i = \hat{\boldsymbol{m}} + \left(\sqrt{(n+\lambda)\boldsymbol{P}^m}\right)_i, \text{ for } i = 1 : n \tag{14}$$

$$\boldsymbol{\mathcal{M}}_{n+i} = \hat{\boldsymbol{m}} - \left(\sqrt{(n+\lambda)\boldsymbol{P}^m}\right)_i, \text{ for } i = 1 : n. \tag{15}$$

The parameter λ remains free for tuning in order to adjust the spread of the sigma-points about the predicted mean estimate in directions of principle variances. It is suggested to select $n+\lambda = 3$ if $\boldsymbol{m}$ is Gaussian [8]. The notation $(\cdot)_i$ denotes the i-column of the matrix within parentheses. Each sigma-point is associated with a weight defined as in Eq. 16.

$$W_0 = \frac{\lambda}{n+\lambda}, W_i = W_{i+n} = \frac{1}{2(n+\lambda)}, \text{for } i = 1:n. \tag{16}$$

The misfit measures for all r output measurements are obtained by mapping the sigma-points through the misfit functional of Eq. 12. The mapping for r multiple receivers $\boldsymbol{s} = (s_1, s_2, \ldots, s_r)$, $\boldsymbol{s} : \mathbb{R}^n \mapsto \mathbb{R}^r$, is done for each sigma-point as written in Eq. 17.

$$\boldsymbol{\mathcal{S}}_i = \boldsymbol{s}\left(\mathcal{M}_i\right), \text{for } i = 0:2n. \tag{17}$$

After the nonlinear mapping of the sigma-points through the nonlinear model, the mean of the predicted misfit $\hat{\boldsymbol{s}}$, covariance of the predicted parameters $\boldsymbol{P}^m$, covariance of the misfit at the predicted model $\boldsymbol{P}^s$, and cross-covariance between them $\boldsymbol{P}^{ms}$ are approximated by weighted summation rule as follows:

$$\hat{\boldsymbol{s}} = \sum_{i=0}^{2n} W_i \boldsymbol{\mathcal{S}}_i, \tag{18}$$

$$\boldsymbol{P}^m = \sum_{i=0}^{2n} W_i \left(\boldsymbol{\mathcal{M}}_i - \hat{\boldsymbol{m}}\right)\left(\boldsymbol{\mathcal{M}}_i - \hat{\boldsymbol{m}}\right)^t + \boldsymbol{Q}, \tag{19}$$

$$\boldsymbol{P}^s = \sum_{i=0}^{2n} W_i \left(\boldsymbol{\mathcal{S}}_i - \hat{\boldsymbol{s}}\right)\left(\boldsymbol{\mathcal{S}}_i - \hat{\boldsymbol{s}}\right)^t + \boldsymbol{R}, \tag{20}$$

$$\boldsymbol{P}^{ms} = \sum_{i=0}^{2n} W_i \left(\boldsymbol{\mathcal{M}}_i - \hat{\boldsymbol{m}}\right)\left(\boldsymbol{\mathcal{S}}_i - \hat{\boldsymbol{s}}\right)^t. \tag{21}$$

Posterior mean $\hat{\boldsymbol{m}}_+$ and covariance $\boldsymbol{P}^m_+$ of the estimated model parameters are updated following the Kalman filter's measurement update step:

$$\hat{\boldsymbol{m}}_+ = \hat{\boldsymbol{m}} + \boldsymbol{K}\left(\boldsymbol{0} - \hat{\boldsymbol{s}}\right) \tag{22}$$

$$\boldsymbol{P}^m_+ = \boldsymbol{P}^m - \boldsymbol{K}\boldsymbol{P}^s\boldsymbol{K}^t \tag{23}$$

with the Kalman gain $\boldsymbol{K}$ calculated as

$$\boldsymbol{K} = \boldsymbol{P}^{ms}\left(\boldsymbol{P}^s\right)^{-1}. \tag{24}$$

To initialize the UKF procedure, some prior knowledge about the model is provided in form of Gaussian distribution $\rho_0(\boldsymbol{m}) \sim \mathcal{N}(\boldsymbol{m}_0, \boldsymbol{P}_0)$. In the first iteration of the UKF, this prior information is assigned to the predicted mean and covariance: $\hat{\boldsymbol{m}} = \boldsymbol{m}_0$, and $\boldsymbol{P} = \boldsymbol{P}_0$. In the successive iterations, the predicted estimated mean and covariance are updated by taking the respective values from the posterior estimate, i.e. $\hat{\boldsymbol{m}} = \boldsymbol{m}_+$ and $\boldsymbol{P} = \boldsymbol{P}_+$.

Described UKF procedure for minimizing the misfit functional locally has been successfully implemented within the hybrid algorithm combined with simulated annealing in the global optimization procedure with implementation in full waves inversion [11].

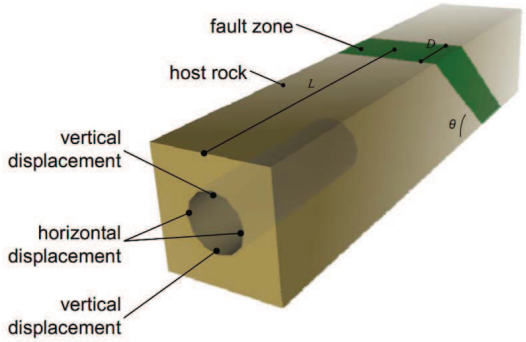

a)

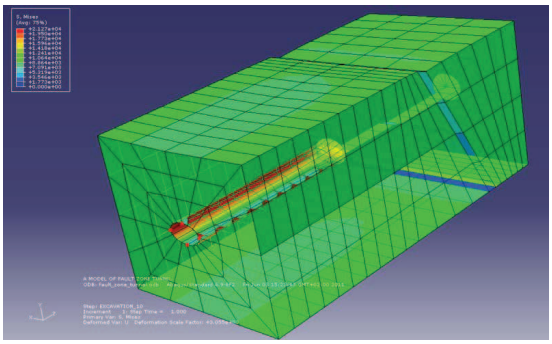

b)

Figure 1: a) 3D tunnel excavation with a fault zone ahead of tunnel face [12] and b) FE model

	Host rock	Fault zone
$E[kN/m^2]$	2×10^8	5×10^7
ν	0.2	0.35
$\rho[kg/m^3]$	2500	2200

Table 1: Material parameters

3 IMPLEMENTATION OF KALMAN FILTERS

Following numeric examples demonstrate efficient implementation of the inversion methods based on Kalman filtering techniques for the parmeter estimation in geotechnical and tunneling problems.

3.1 3D tunnel excavation: EKF identification of geometrical and elastic material parameters

In this numeric example the EKF is used for estimation of both material and geometrical parameters of a 3D tunnel excavation model [12] depicted in Figure 1 a). The model represents a mountain cut-out with overburden height of 500 meters. Dimensions of the model are $100m \times 100m \times 200m$. A fault zone is located at L meters from the model frontal face measured from its top edge having a thickness of D meters. The fault dip direction and the angle of 66° of inclination are supposedly known from an engineering-geology investigation.

The material parameters are given in Table 1. The initial geostatic stresses are imposed with prescribed horizontal stress to vertical stress ratio equal to 1, i.e. $\sigma_h = \sigma_v$. To account for this model feature, a surface pressure of $1.23 \times 10^4\ kN/m^2$ is applied on the top side of the model. This value is calculated assuming the overburden rock mass to be homogeneous, with a density of 2500 kg/m^3. The displacement history data are collected during the simulation of 10 tunnel excavations, each of 10 meters length. Observation points are located at the tunnel crown, bottom and at the side walls. A 3D finite element tunnel excavation model built with ABAQUS is presented in Figure 1 b). The elements in the tunnel are 6-node triangular prism elements (5-sided), and rest of the soil body elements are 8-node brick elements (6-sided). The state vector contains three components: one material parameter – Young's modulus *E* and two geometrical parameters – *L* and *D* as depicted in Figure 1.

$$x = \left[\begin{array}{ccc} L[m] & D[m] & E[kN/m^2] \end{array} \right]$$

Convergence of the algorithm was investigated for different initial state estimate vectors and it

was shown that the convergence rate varies with the initial guess. Results for two cases of initial state vectors are presented in Tables 2 and 3.

Parameter	Initial state	Estimated state	Deviation from true state
L[m]	130	119.70	0.30
D[m]	10	6.01	0.01
E[kN/m^2]	4.0×10^7	5.03×10^7	0.03×10^7

Table 2: Converged result after 15 iterations - Case 1

Parameter	Initial state	Estimated state	Deviation from true state
L[m]	115	120.32	0.32
D[m]	4	5.99	0.01
E[kN/m^2]	4.0×10^7	4.96×10^7	0.04×10^7

Table 3: Converged result after 20 iterations - Case 2

Graphical results of the progressing Kalman filter for Case 1 are shown in Figure 2.

3.2 Implementation of SPKF for model calibration of soil parameters in mechanized tunneling

Geomechanical analysis of tunnel excavation in this example can be considered as a quasi-static non-Markov process, i.e. the state of the model is about equilibrium along the analysis and the current state depends not only on the previous state but also on the history of analysis steps. The model of a shield tunnel boring machine (TBM) advancing in homogeneous soil, Fig. 3, obtained using the FEA software PLAXIS 3D was provided by the C2-subproject within the Collaborative Research Center SFB 837 at the Ruhr University Bochum [14]. The model domain is 60 m long, 40 m wide, and 45 m deep. The tunnel of diameter D = 8.5 m and under an overburden depth equal to 1D. Except that the ground surface is stress-free, all other boundaries of the FE model are constrained by zero displacements. Only a half of the model is analyzed because of the symmetric geometrical, loading and material conditions about the vertical plane along the tunnel axis. The homogeneous soil behaves according to the Hardening Soil constitutive model in [13].

The set of parameters chosen for identification, with their assumed 'true' values for the forward simulation includes stiffness for un-/reloading $G_{ur} = 41600[kN/m^2]$, secant stiffness in standard drained triaxial test $E_{50} = 35000[kN/m^2]$, and friction angle $\phi = 35[°]$. Observation positions and orientations at observation surface at 39 m from beginning position of the tunnel head (before excavation) and perpendicular to the tunnel axis are depicted in Fig. 3. The model is calculated for 30 excavation steps, each step advances the TBM 1.5 m forward. Calculated outputs obtained from the FE model are registered at every excavation step. Synthetic measurement data are assumed with additive Gaussian noise with standard deviations of 3% and 5% the mean value of the noise-free FE calculated outputs for each measurement point. The feasible ranges for the considered soil parameters are defined such that the lower bounds and upper bounds are considerably distant from true parameters: $20833 \leq G_{ur}$[kN/m^2] ≤ 62499, $17500 \leq E_{50}$[kN/m^2] ≤ 52500 and $32 \leq \phi[°] \leq 52.5$. Taking into account the assumption

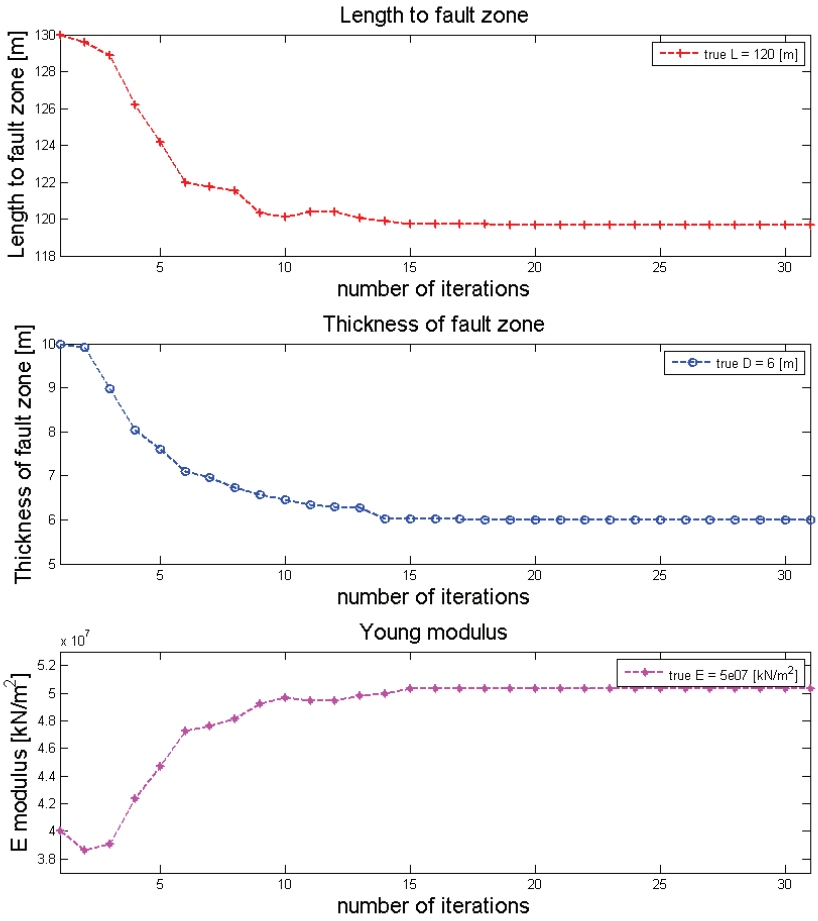

Figure 2: Graphical result convergence of the estimated parameters - initial case 1

that the parameters are uncorrelated, the initial state error covariance matrix for the parameters $\mathbf{m} = [G_{ur}; \phi; E_{50}]$ is set: $\mathbf{P}(0|0) = \text{diag}\left(4000^2, 5^2, 5000^2\right)$. The authors' practice for setting the covariance matrix of the process noise $\mathbf{Q}$ is that it can be set in such a way that its square roots are ranging from five percent to ten percent the values of initial estimation error standard deviations. In this work, it is chosen to be around seven percent, i.e. the covariance matrix of the process noise can be set as $\mathbf{Q} = 0.005\mathbf{P}_0$. For setting up the nonlinear Kalman filters in this study, every measurement datum is assigned to have the same covariance, i.e. $\mathbf{R} = 0.01^2 * \mathbf{I}(m, m)$, with $\mathbf{I}(m, m)$ the identity matrix having dimension equal to the size of the measurement data, m.

Selected comparison results of the EKF and SPKF with initial parameters chosen at the extremes of feasible ranges are presented in Table 4 and Table 5 for cases of 3% and 5% measurement noise, respectively.

Graphical plots of the converging soil parameters in Fig. 4 demonstrate fast and robust convergence. The investigation has shown, that depending on the initially selected parameter values, the convergence of the SPKF can require less itteration steps than for the EKF.

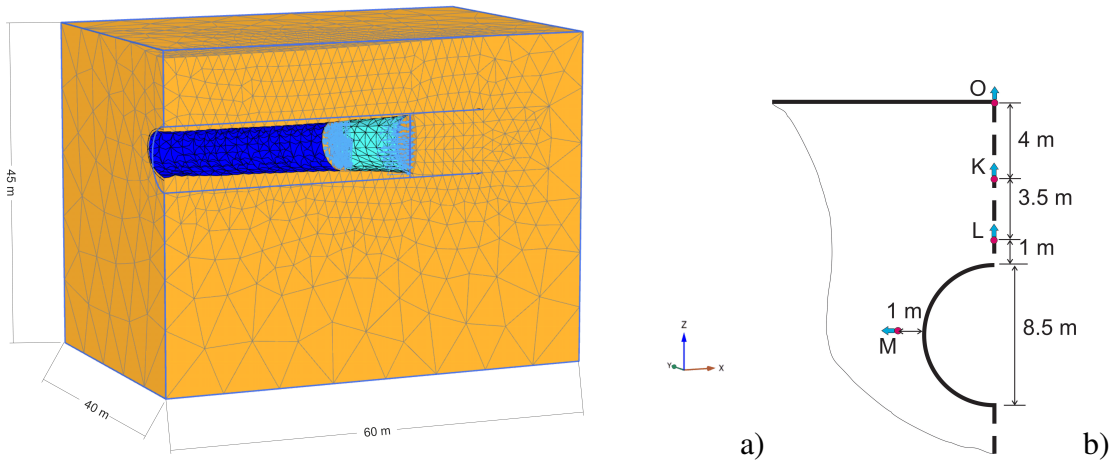

Figure 3: a) FE model of the 3D tunnel excavation and b) Measurement points at observation section

Parameter	Initial		EKF		SPKF	
	Mean	SD	Mean	SD	Mean	SD
G_{ur}[kN/m^2]	20833	4000	41588.02	552.30	41476.61	296.64
E_{50}[kN/m^2]	17500	5000	34856.67	958.45	34643.40	387.50
ϕ[°]	32	5	34.96	0.25	34.91	0.35

Table 4: Identified soil parameters with 3% measurement noise

Parameter	Initial		EKF		SPKF	
	Mean	SD	Mean	SD	Mean	SD
G_{ur}[kN/m^2]	20833	4000	42483.47	6317.98	42288.64	392.62
E_{50}[kN/m^2]	17500	5000	37036.86	1130.50	36646.55	600.89
ϕ[°]	32	5	35.52	2.82	35.42	0.37

Table 5: Identified soil parameters with 5% measurement noise

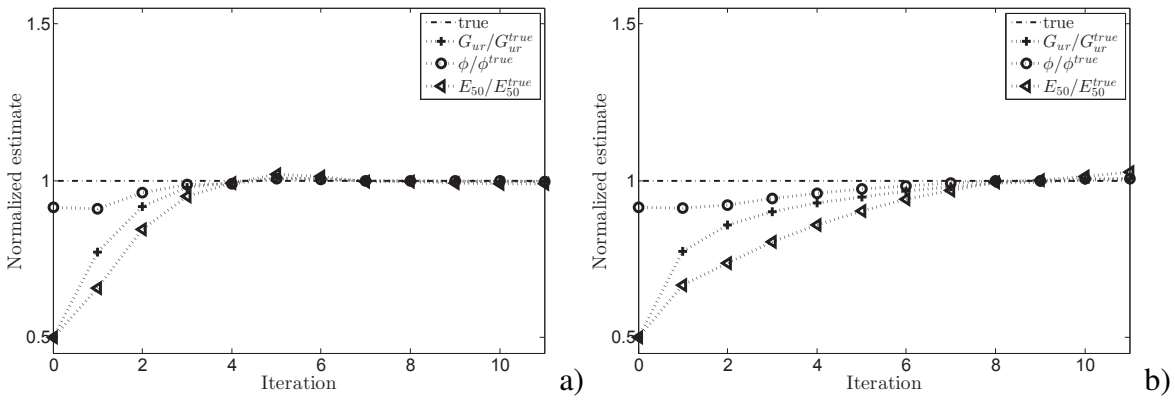

Figure 4: Iterative development of soil parameters with a) 3% and b) 5% measurement noise SPKF

4 Conclusions

Good convergence of the parameter estimation shown through examples of geotechnical problems presented in this work has proven that the Kalman filtering techniques have prospects to be a reliable method for parameter identification in geotechnical engineering. An important advantage of the Kalman filters, utilization of the measurement uncertainties, which cannot be avoided in large scale geotechnical structures, makes it a very attractive and powerful estimation method, which performs well even in the environment corrupted by noise. Another prominent advantage is that the choice of initial model parameters must not be very close to the true parameter set as for other gradient-based optimization methods. Implementation of the Kalman filters, relating the implementation effort in comparison with the resulting outcome, represents relatively simple, but still a very powerful tool, since using modern programming languages the Kalman filter algorithm can be realized within several code lines including vector and matrix manipulations. However, the tuning and adjusting the filter's configurations plays a decisive role regarding its successful implementation and therefore requires a special attention. Good understanding of the model and the influence of each parameter on the model is crucial for the configuration of the Kalman filter in order to achieve its successful convergence.

Acknowledgements

The authors gratefully acknowledge the funding by the German Research Foundation (DFG) within Collaborative Research Center under grant SFB-837/A2.

REFERENCES

[1] R.E. Kalman, A New Approach to Linear Filtering and Prediction Problems, *Trans. ASME*, Ser. D: J. Basic Eng. **82**, 35-45, 1960.

[2] M. Hoshiya, A. Suto, Kalman Filter - Finite Element Method in Identification, *Journal of Engineering Mechanics* **119**:2, 197-210, 1993.

[3] A. Murakami, *Studies on the Application of Kalman Filtering to some Geomechanical Problems Related to Safety Assessment*, doctoral dissertation, Kyoto University, 1991.

[4] Wang Yang, *Extended Kalman Filter Method for Parameter Identification and its Application in Tunneling*, doctoral dissertation, Universität Innsbruck, 2004.

[5] L.T. Nguyen, M. Datcheva, T. Nestorović, Identification of a fault zone ahead of the tunnel excavation face using the extended Kalman filter, *Mechanics Research Communications*, **53**, 47-52, 2003.

[6] A. Gelb (ed.), *Applied Optimal Estimation*, MIT Press, Cambridge, Massachusetts, 1974.

[7] D. Simon, *Optimal State Estimation - Kalman, H_∞ and Nonlinear Approaches*. John Wiley & Sons, 2006.

[8] S.J. Julier, J.K. Uhlmann, A new extension of the Kalman filter to nonlinear systems, *Proc. AeroSense: 11th Int. Symp. Aerospace/Defense Sensing, Simulation and Controls*, 182-193, 1997.

[9] R. Van Der Merwe, *Sigma-point Kalman filters for probabilistic inference in dynamic state-space models*, doctoral dissertation, Oregon Health & Science University, 2004.

[10] R. Kandepu, L. Imsland, B.A. Foss, Constrained state estimation using the unscented Kalman filter, *Proceedings of the 16th Mediterranean Conference on Control and Automation*, 1453-1458, 2008.

[11] L.T. Nguyen, T. Nestorović, Unscented hybrid simulated annealing for fast inversion of tunnel seismic waves, *Computer Methods in Applied Mechanics and Engineering*, **31**, 281-299, 2016.

[12] J. Meier, M. Datcheva, T. Schanz, Identification of Constitutive and Geometrical Parameters of Numerical Models with Application in Tunneling, *EURO:TUN, Vienna*, 2007.

[13] T. Schanz, P.A. Vermeer, P.G. Bonnier, The hardening-soil model: Formulation and verification, *Beyond 2000 in Computational Geotechnics*, Balkema, Rotterdam, 281-290, 1999.

[14] V. Zarev, T. Schanz, M. Datcheva, Three-dimensional finite-element analysis of mechanized shield tunneling in urban areas, *Proceedings of The Thirteenth International Conference on Civil, Structural and Environmental Engineering Computing*, Greece 1-10, 2011.